Lowest-order corrections to the RPA polarizability and GW self-energy of a semiconducting wire

Lowest-order corrections to the RPA polarizability and *GW* self-energy of a semiconducting wire

H. J. de Groot, R. T. M. Ummels, P. A. Bobbert, and W. van Haeringen
Department of Applied Physics, Eindhoven University of Technology, P.O. Box 513, 5600 MB Eindhoven, The Netherlands
(Received 16 February 1996)

We present the results of the addition of lowest-order vertex and self-consistency corrections to the RPA polarizability and the *GW* self-energy for a semiconducting wire. It is found that, when starting from a local density approximation zeroth-order Green function and systematically including these corrections in *both* the polarizability and the self-energy, the correction to the non-self-consistent RPA-*GW* band gap is small. Partial inclusion of these corrections leads to very different band gaps. This sheds new light on the puzzling question why non-self-consistent RPA-*GW* calculations of band gaps have been so very successful. [S0163-1829(96)07128-7]

I. INTRODUCTION

The present work was stimulated by the results of a previous paper,[1] in which self-consistent RPA-*GW* calculations were presented, for a quasi-one-dimensional model semiconductor (semiconducting wire). For this model quantum Monte Carlo (QMC) calculations were performed by Knorr and Godby[2,3] (KG). In Ref. 1 very large values were obtained, as compared to the results of these QMC calculations, for energy band gaps. This has led to a puzzling situation. On the one hand, the gap values obtained by KG are expected to be exact in principle, within the statistical uncertainties. On the other hand, the self-consistent *GW* band-gap results in Ref. 1 are reliable (from now on we will often omit the prefix RPA, when we talk about RPA-*GW*, and will simply call it *GW*). The reason why the self-consistent *GW* results are to be trusted lies in the fact that it is convincingly shown that precisely the same self-consistent gap values result when completely different starting situations are chosen in the iteration cycle leading to self-consistency. The discrepancy is therefore very likely due to an intrinsic difference between the ''exact'' or QMC-treated interacting system of electrons and a system for which *GW* is brought to full self-consistency. As vertex corrections, both to the self-energy M and to the polarizability P, are missing in a self-consistent *GW* treatment, we will focus in this work on the question of whether indeed those missing corrections can be held responsible for the discrepancy.

The strategy in this paper is to start from the ''best'' available electron Green function G, which is the density functional (DFT) Green function in the local density approximation (LDA), and screened interaction W, which is the RPA screened interaction, and systematically calculate higher-order corrections. It is of interest to note that the non-self-consistent *GW* self-energy calculated with these G and W leads to gap values that are comparable to those of KG (see, however, the remarks at the end of Sec. III). In *GW* calculations for actual three-dimensional systems this procedure leads to gaps that are in excellent agreement with experiment. We will particularly focus on the addition to the *GW* self-energy (first order in the screened interaction W) of lowest-order vertex corrections (second order in W). We will also add self-consistency (SC) corrections to M, again to second order in W. For reasons of consistency[4] we will add similar corrections to the polarizability P. The results of these additions will possibly enable us to identify the origin of the discrepancy between the treatments in Refs. 1, 2, and 3 as it is not unlikely (see below) that vertex corrections and sc corrections will cancel to a large extent.

We emphasize that from a fundamental point of view it is in fact obligatory to include vertex and SC corrections *simultaneously* to the same order in the screened interaction W. It was already noted by Kohn[5] that, for instance, for the polarizability P in an insulator, the inclusion of *both* vertex and SC Feynman diagrams is necessary in order to obtain the correct quadratic behavior in the static polarizability $P(k)$, if the wave vector $k \rightarrow 0$. We will encounter this again in the treatment of our model system.

Inclusion of vertex corrections and SC effects has been studied earlier by many researchers, mainly if not exclusively, however, for the homogeneous electron gas. We are not aware of precise evaluations of *both* types of corrections for insulating or semiconducting systems. All results in the homogeneous electron gas case seem to indicate that the two contributions have a tendency to cancel each other. DuBois[6,7] stresses the importance of taking into account all diagrams of the same order in the Wigner-Seitz radius r_s for the polarizability, both vertex and SC diagrams. These contributions appeared to cancel to a large extent. Geldart and Taylor[8,9] found for the homogeneous electron gas a cancellation of the logarithmically divergent contributions of vertex and SC corrections to the static polarizability $P(k)$ for $k \rightarrow 0$, leaving only a constant contribution. Minnhagen[10] noted that inclusion of the lowest-order vertex correction in P and M had little effect on the position of the quasiparticle peaks for the homogeneous electron gas. In accordance with this, Mahan and Sernelius[11] observed that the effects on the bandwidth of a homogeneous electron gas due to the addition of vertex corrections to P and M nearly cancel. Hong and Mahan[12] observed that the SC corrections tend to decrease P, whereas the vertex corrections tend to increase P. The necessity to take into account the correct combination of vertex and SC diagrams is further stressed by Mahan[13] in his review of several *GW* approximations. Engel and Vosko[14] have given an analytic derivation of the exchange contribution to the response function of the homogeneous electron

gas. In their treatment they confirm the above quoted results of Geldart and Taylor concerning the cancellation of divergent contributions to P.

As far as the insulating or semiconducting case is concerned there has been little well-established evidence for cancellation effects until now. This is mainly due to the difficulty of evaluating the corrections. It is only quite recently that we were able to carry through reliable procedures to evaluate the additional required diagrams. Daling and van Haeringen[15] calculated the lowest-order vertex correction diagram (lowest order in the *bare* Coulomb interaction) to the self-energy in the case of the semiconductor silicon and found the correction to the energy gap to be less than about 0.1 eV. Bobbert and van Haeringen[16] repeated this calculation, by using the *screened* interaction instead of the bare one. Again a small but not entirely insignificant contribution was obtained. Incidentally, the treatment of Ref. 16 is presently being completed by us with the inclusion of the SC corrections to the same order in W.

Finally, the effects of improving G and W in GW calculations of a Hubbard cluster were investigated by Verdozzi, Godby, and Halloway[17] by comparing to the exact result that can be obtained in this case. It was found that with the density functional G and RPA W in the GW self-energy better results were obtained than with the exact G and W, concluding that vertex corrections should be included in the latter case.

All of the above-mentioned studies seem thus to confirm or at least suggest that vertex and SC corrections, if taken to the same order in the interaction, cancel to a large extent, though the evidence for the case of insulating or semiconducting systems is less well established than for the homogeneous electron gas case.

In view of the above quoted fully self-consistent GW calculations and the large difference between the thus obtained gaps and those in the QMC treatment of KG, the leading idea in the present paper is to investigate for a model system if indeed the vertex corrections to non-self-consistent GW cancel the additional SC corrections, such that we can better understand how a *totally* self-consistent GW calculation might lead to gap results that are completely at odds with the QMC-obtained results. It could eventually give support to the view that non-self-consistent GW is to be preferred over self-consistent GW.

In Sec. II we give a short description of the involved quasi-one-dimensional model and describe which Feynman diagrams we take into account for the calculation of P and M. In Sec. III we give the results of the vertex and SC corrections to the band gap, and discuss and relate them to the fully self-consistent GW results, and to the results of KG. Expressions attributed to the involved higher-order diagrams for P and M are given in the Appendix.

II. THE MODEL AND THE CALCULATED DIAGRAMS

In this section, we briefly describe the quasi-one-dimensional model for which all present calculations are performed. For a more detailed description of the model we refer to either Ref. 3 or Ref. 1. Furthermore, we discuss which diagrams we include in our calculations of P and M.

In the quasi-one-dimensional model that we use the electrons are confined to a line by a strong lateral potential in the x and y directions, $V(x,y)=\gamma^4(x^2+y^2)/2$, where γ is the strength of the potential, taken to be $4\pi/a$. Atomic units are used. In the z direction, the electrons are subject to an external potential of the form $V^{\rm ext}(z)=A\cos(2\pi z/a)$, where A is the strength of the potential and a is the lattice constant, which we have chosen to be 5 a.u. In reciprocal space, the one-dimensional Coulomb interaction reads

$$v_{K_1,K_2}(k)=\exp\left[\frac{1}{2}\left(\frac{k+K_1-K_2}{\gamma}\right)^2\right]E_1\left[\frac{1}{2}\left(\frac{k+K_1-K_2}{\gamma}\right)^2\right], \tag{1}$$

where E_1 is the exponential integral, and K_1 and K_2 are reciprocal lattice vectors. $v(k)$ diverges logarithmically for $K_1-K_2=0$ and $k\to 0$, and in the large k limit $v(k)$ is proportional to k^{-2}. In real space the model Coulomb interaction is finite for $z=0$, and behaves as z^{-1} if $z\to\infty$, where z is the interelectronic distance.

We first calculate the zeroth-order LDA Green function G^0, which is of the form

$$G^0_{K_1,K_2}(k,\epsilon)=\sum_l \frac{d^{0\,*}_{l,K_1}(k)d^0_{l,K_2}(k)}{\epsilon-\epsilon^0_l(k)+i\,\eta\,\mathrm{sgn}[\epsilon^0_l(k)-\mu]}, \tag{2}$$

where ϵ is the energy. The sum is over the energy bands l, and the chemical potential μ is chosen somewhere in the energy gap of the semiconductor. The quantity η is infinitesimally small and positive. The poles in Eq. (2) can be associated with electrons in either a valence band or holes in a conduction band, depending on $\mathrm{sgn}[\epsilon^0_l(k)-\mu]$ being negative or positive. The $d^0_{l,K}(k)$'s and the $\epsilon^0_l(k)$'s are the normalized eigenvector coefficients and eigenvalues, respectively, following from the band-structure equation

$$[\tfrac{1}{2}(k+K_1)^2-\epsilon^0_l(k)]d^0_{l,K_1}(k)+\sum_{K_2}[V^{\rm ext}_{K_1,K_2}+V^{\rm H}_{K_1,K_2}+V^{\rm XC}_{K_1-K_2}]d^0_{l,K_2}(k)=0, \tag{3}$$

in which V^H is the Hartree potential, and $V^{\rm XC}$ is the exchange-correlation potential in the LDA. With G^0 we calculate the RPA polarizability $P^{\rm RPA}$, the expression of which is given by Eq. (5) of Appendix, and which is depicted as a Feynman diagram in Fig. 1. The corresponding screened interaction is found from

$$W^{-1}_{K_1,K_2}(k,\epsilon)=v^{-1}_{K_1,K_2}(k)-P_{K_1,K_2}(k,\epsilon), \tag{4}$$

where v^{-1} is the inverse of the effective one-dimensional Coulomb interaction. We use G^0 and $W^{\rm RPA}$ as inputs for the calculation of the higher-order corrections to P. We write $W=v+\tilde{W}$, where $\tilde{W}$ is the screening part of the screened interaction. We use an energy representation for $\tilde{W}$ in terms of simple poles,[18,1] with ten poles per k value. With pole representations for G^0 and W it is possible to analytically perform the energy integrations that arise in the expressions of the diagrams contribution to P and M that we want to calculate. For the k integrations we take 64 points in the first Brillouin zone, which we choose to be $[0,2\pi/a]$, and we take into account four energy bands, one valence band and

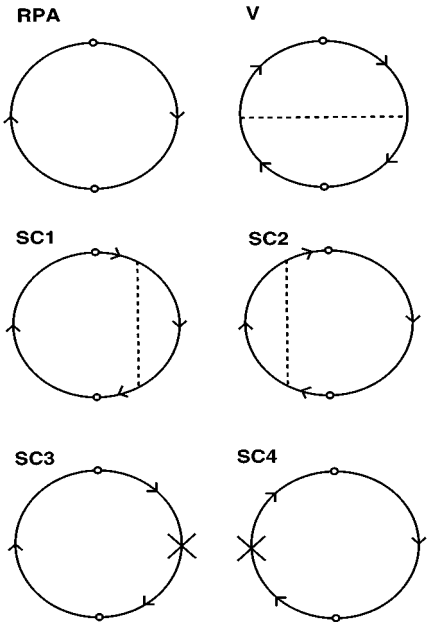

FIG. 1. The Feynman diagrams included in the polarizability P. Diagram RPA is the RPA polarizability, diagram V denotes the lowest-order vertex correction contribution, and diagrams SC1 to SC4 are the lowest-order self-consistency contributions. The solid directed line denotes the LDA electron Green function G^0, and the dashed line denotes the RPA screened interaction W. The cross in diagram SC3 and SC4 denotes $-V^{\mathrm{XC}}$.

three conduction bands, and four plane waves $K=-4\pi/a,-2\pi/a$, and $0,2\pi/a$. A few subdiagrams, for P as well as for M, were calculated with six plane waves and six energy bands and the effect on the band gap was found to be of the order of 1%, indicating that the total error in the band gap is of the order of a few percent. The amount of computer time needed for the calculations scales as the square of the number of plane waves times the cube of the number of energy bands. Performing all calculations for six plane waves and six energy bands would require an excessive amount of computer time (several months on a Silicon Graphics Power Challenge).

The RPA polarizability as well as the higher-order diagrams that we include in our calculation for P are depicted in Fig. 1. Diagram V of Fig. 1 is the lowest-order vertex correction diagram, and diagrams SC1 to SC4 of Fig. 1 are the lowest-order self-consistency diagrams. The cross in diagram SC2 of Fig. 1 denotes the negative of the exchange-correlation potential V^{XC}. This diagram should be included when using an LDA G^0, because V^{XC} is already included in G^0, and we must avoid double counting. The expressions pertaining to diagrams V and SC1 to SC4 of Fig. 1 are given in Eqs. (A2)–(A4).

In the Appendix we give the general expressions for the diagrams of Fig. 1. Note that the diagrams V, SC1, and SC2 are of the same order in W. Kohn[5] showed that diagrams contributing to P, in which two intraband transitions occur, go to a constant when $k\rightarrow 0$. He also found that the constant contribution of a certain diagram with two intraband transitions always cancels against the constant contribution of another diagram with two intraband transitions, leaving a contribution to P that is quadratic in k. To first order in W this means that the constant contribution from the vertex correction diagram cancels that of the self-consistency diagrams.

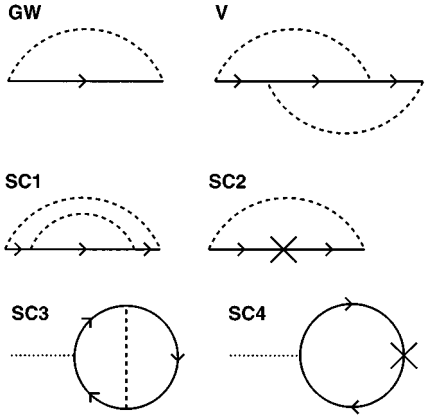

FIG. 2. The diagrams included in the self-energy M. Diagram GW is the GW self-energy, diagram V denotes the lowest-order vertex correction contribution, and diagrams SC1 to SC4 are the lowest-order self-consistency contributions to the self-energy. The dashed line now denotes the screened interaction W obtained with one of the four choices for the polarizability P mentioned in the text. The dotted line in diagrams SC3 and SC4 denotes the bare Coulomb interaction.

We add the higher-order corrections to P^{RPA}, and construct a new W according to Eq. (4). At this point we want to consider four different screened interactions that we subsequently try as an input to the calculation of the self-energy diagrams. They follow from (1) P^{RPA}, the RPA polarizability (diagram RPA of Fig. 1); (2) $P^{\mathrm{RPA}}+P^{V}$, the RPA polarizability plus vertex corrections to P (diagrams RPA and V of Fig. 1); (3) $P^{\mathrm{RPA}}+P^{\mathrm{SC1}}+P^{\mathrm{SC2}}+P^{\mathrm{SC3}}+P^{\mathrm{SC4}}$, the RPA polarizability plus self-consistency corrections to P (diagrams RPA and SC1 to SC4 of Fig. 1); (4) $P^{\mathrm{RPA}}+P^{V}+P^{\mathrm{SC1}}+P^{\mathrm{SC2}}+P^{\mathrm{SC3}}+P^{\mathrm{SC4}}$, the RPA polarizability plus vertex plus self-consistency corrections to P (all diagrams of Fig. 1).

The GW self-energy diagram and the higher-order diagrams for the self-energy M are depicted in Fig. 2. Diagram GW of Fig. 2 is the well-known GW self-energy, diagram V is the lowest-order vertex correction diagram, and the other diagrams are the lowest-order self-consistency diagrams. Again, the vertex correction diagram and the self-consistency diagrams are of the same order. Diagrams SC3 and SC4 of Fig. 2 are corrections to the Hartree diagram, and can be thought of as being self-energy corrections due to higher-order corrections to the electron density. The general expressions for the diagrams of Fig. 2 are given in the Appendix.

Analogously to the polarizability, we want to consider various combinations of diagrams to be included in the self-energy: (1) M^{GW}: the GW self-energy (diagram GW of Fig. 2). (2) $M^{GW}+M^{V}$: the GW self-energy plus vertex corrections (diagrams GW and V of Fig. 2). (3) $M^{GW}+M^{\mathrm{SC1}}+M^{\mathrm{SC2}}+M^{\mathrm{SC3}}+M^{\mathrm{SC4}}$: the GW self-energy plus self-consistency corrections (diagrams GW and SC1 to SC4 of Fig. 2). (4) $M^{GW}+M^{V}+M^{\mathrm{SC1}}+M^{\mathrm{SC2}}+M^{\mathrm{SC3}}+M^{\mathrm{SC4}}$: the GW self-energy plus vertex corrections plus self-consistency corrections (all diagrams of Fig. 2).

TABLE I. Gaps (in atomic units) for different combinations of vertex (V) and self-consistency (SC) corrections to the self-energy M and polarizability P, calculated with an LDA G^0, for $A=0.15$. The LDA gap is 0.0400 a.u. The numbers in parentheses are the shifts of the tops of the valence bands compared to the LDA case. The self-consistent RPA-GW result is 0.390 a.u. (Ref. 1). The QMC value of KG is 0.128 ± 0.05 a.u. (Ref. 3).

	P			
M	RPA	RPA + V	RPA + SC	RPA + V + SC
GW	0.0884 (-0.0230)	0.070 (0.045)	0.139 (-0.041)	0.169 (-0.054)
GW + V	0.118 (0.002)	0.154 (0.019)	0.138 (-0.025)	0.153 (-0.044)
GW + SC	0.123 (-0.027)	0.073 (0.023)	0.333 (-0.052)	0.143 (-0.037)
GW + V + SC	0.132 (-0.017)	0.166 (0.020)	0.328 (-0.051)	0.106 (-0.027)

Together with the four different choices that we may make for the screened interaction P, this gives 16 possible combinations for the calculation of the self-energy. In order to calculate the renormalized quasiparticle energies for all these cases, we solve Eq. (3) again, but replace $V^{\mathrm{XC}}_{K_1-K_2}$ by the energy-dependent and nonlocal self-energy $M_{K_1,K_2}(k,\epsilon)$. We drop the superscript 0, and the eigenvalues $\epsilon_l(k,\epsilon)$ now become energy dependent. We calculate $\epsilon_l(k,\epsilon)$ for a few values of ϵ around $\epsilon^0_l(k)$, fit this with a second-order polynomial, and then solve the quasiparticle equation $\epsilon=\epsilon_l(k,\epsilon)$. This turns out to be accurate enough. Although this equation in general has complex solutions, in this paper we will ignore the small imaginary parts and only consider the real parts.

Each possible time order of the internal and external points of the diagrams in Figs. 1 and 2 can be associated with a different subdiagram, which has to be calculated separately. For the vertex correction to the polarizability (diagram V of Fig. 1), we get a total of 30 subdiagrams. This can be seen as follows, keeping in mind that we split W into the bare Coulomb interaction v and the screened part $\widetilde{W}$: there are $6(=3!)$ possible subdiagrams when the interaction is the Coulomb interaction, plus $24(=4!)$ subdiagrams when the screened part of the screened interaction is taken. For diagrams SC1 and SC2 of Fig. 1 there are $2\times30=60$ subdiagrams, and for diagrams SC3 and SC4 of Fig. 1 there are $2\times3!=12$ different subdiagrams.

For the vertex correction diagram to the self-energy (diagram V of Fig. 2) there are 38 different subdiagrams (for more details see Ref. 16). For diagram SC1 of Fig. 2 we also get 38 subdiagrams, for diagram SC2 of Fig. 2 we get $2!+3!=8$ subdiagrams, and for the diagrams SC3 and SC4 of Fig. 2 we find 8 and 2 subdiagrams, respectively.

III. RESULTS AND DISCUSSION

In Tables I and II we present the main results of the present calculations. For each of the above-mentioned possible combinations including vertex and self-consistency effects to the polarizability P and self-energy M we present the calculated band gaps for the model system for two values of the strength of the external potential, $A=0.15$ and $A=0.25$. The upper-left number is the non-self-consistent RPA-GW band gap, which is the same as the first iteration GW band gap in Table II of Ref. 1. The lower-right number is the result of the most complete calculation, including vertex and sc corrections in both P and M. The most striking fact is that this latter number is quite close to the first, contrary to almost all of the other numbers in the table. This means that after inclusion of vertex *and* sc corrections in both P and M the ordinary, non-self-consistent GW result is roughly reproduced.

We investigated the possible cancellation between vertex and self-consistency corrections to P, suggested by Hong and Mahan,[12] by plotting the (0,0) matrix element of the static ($\epsilon=0$) polarizability in Fig. 3. For this situation, there is indeed a clear cancellation between the two corrections. On the one hand, vertex corrections appear to increase the polarizability, having mostly the same sign as the RPA P. On the other hand, self-consistency corrections decrease the polarizability, having mostly the opposite sign compared to the RPA P and vertex corrections to P. These results seem to confirm the cancellation between vertex and sc corrections to P that were found by Hong and Mahan.[12] However, when looking at the gap values in Tables I and II, the trends are equivocal. Vertex corrections and sc corrections in P do not in all cases have an opposite effect to the band gap. This indicates the importance of the other matrix elements and the energy dependence of P.

TABLE II. The same as Table I, but for $A=0.25$. The LDA gap is 0.0750 a.u. The self-consistent RPA-GW result is 0.445 a.u. (Ref. 1). The QMC value of KG is 0.311 ± 0.05 a.u. (Ref. 3).

	P			
M	RPA	RPA + V	RPA + SC	RPA + V + SC
GW	0.1836 (-0.0341)	0.178 (0.019)	0.186 (-0.036)	0.269 (-0.061)
GW + V	0.231 (-0.001)	0.221 (0.012)	0.182 (-0.019)	0.240 (-0.056)
GW + SC	0.316 (-0.041)	0.191 (0.027)	0.350 (-0.039)	0.229 (-0.042)
GW + V + SC	0.287 (-0.028)	0.230 (0.022)	0.341 (-0.038)	0.193 (-0.035)

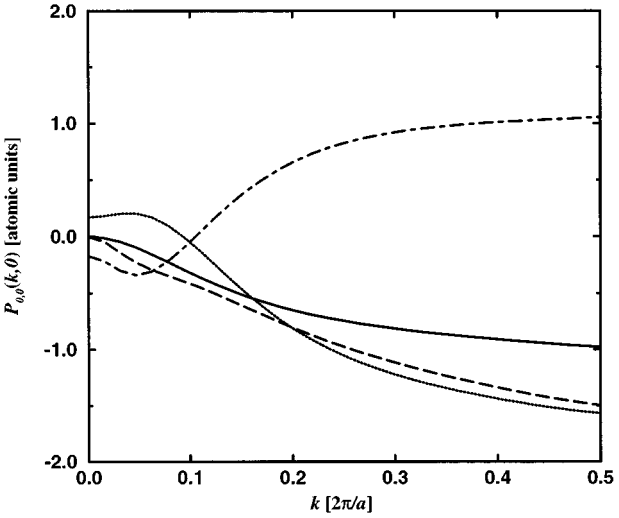

FIG. 3. The RPA (solid line), lowest-order vertex (dotted line), lowest-order self-consistency (dashed-dotted line) and total (dashed line) contributions to the (0,0) matrix element of the static ($\epsilon=0$) polarizability, as a function of the wave vector k, all calculated with the LDA G^0 for the case $A=0.15$.

We reproduce the results of Kohn for the $k\rightarrow 0$ dependence of the static polarizability, because we found that, when $k\rightarrow 0$, the constant contribution to P from the vertex correction diagram exactly cancels the constant contribution from the self-consistency diagrams, leaving the correct quadratic dependence on k as $k\rightarrow 0$ (see also Fig. 3).

We believe that the large self-consistent GW band gap[1] can now be understood in the light of the present calculations of the considered higher-order diagrams. It can be seen in Tables I and II that the effect of adding self-consistency corrections to the RPA P and the GW M is that the band gap increases, in agreement with the band gap after two GW iteration steps. For $A=0.15$ the present calculations give a gap of 0.333 a.u. for the combination [P: RPA+SC; M: GW+SC] (see Table I), compared to a gap of 0.316 a.u. after the second GW iteration step.[1] For $A=0.25$, the corresponding values are 0.350 (see Table II) and 0.387, respectively. The small differences are explained by the fact that in the present calculations we take into account only the lowest-order self-consistency diagrams, whereas in the self-consistent GW iteration cycle we take into account an infinite sum of self-consistency diagrams.

Not all of the combinations in Tables I and II have a clear interpretation, such as, e.g., the band gap resulting from a P in which only vertex corrections are taken into account, and an M with only sc corrections. For completeness, however, we have included the results of those calculations.

In Tables I and II we also give the shift of the top of the valence band compared to the LDA value (the numbers between brackets). We see that the shift of the most complete result is almost equal to the shift of the non-self-consistent RPA-GW result. This means that the cancellations do not only occur for energy differences but also for absolute energies.

The effects on the quasiparticle energies of vertex and self-consistency corrections to P and M have also been calculated at $k=0$ (the boundary of the Brillouin zone) and

TABLE III. Gaps, in a.u., for the LDA, RPA-GW, and the most complete case (vertex and SC corrections in P and M) for the k values 0, $\pi/2a$, and π/a, for the case $A=0.15$. The numbers in parentheses are the shifts of the valence band compared to the LDA case at the particular k point.

	LDA	RPA-GW	Most complete
$k=0$	0.7886	0.7563 (0.0032)	0.754 (0.004)
$k=\pi/2a$	0.3969	0.3971 (-0.0079)	0.401 (-0.005)
$k=\pi/a$	0.0400	0.0884 (-0.0230)	0.106 (-0.027)

$k=\pi/2a$ (halfway to the boundary and the center of the Brillouin zone). The results of these calculations are given in Tables III and IV. The corrections to the band gap, and to the top of the valence band, of the most complete calculations (vertex and SC corrections to both P and M) compared to the non-self-consistent RPA-GW values, are even smaller for $k=0$ and $k=\pi/2a$, than for $k=\pi/a$.

For comparison, we calculated the vertex and self-consistency corrections to P and M with a Hartree-Fock G^0. In that case the cancellation between vertex and self-consistency corrections is less prominent, and the most complete calculation (vertex and self-consistency corrections to both P and M) results in a band gap that goes in the right direction (becomes smaller) but is still far from the band gaps starting from the LDA G^0, illustrating again that it is wise to start from LDA as a zeroth-order result.

Comparing our band gaps to those of KG, we observe that for $A=0.15$ both our RPA-GW band gap and the band gap including vertex and SC corrections (0.0884 and 0.106 a.u., respectively) lie below the value given by KG, but within their error bar (0.128 ± 0.05 a.u.). For $A=0.25$, on the other hand, our values are lower than the KG values but outside the error bar (0.1836 and 0.193 versus 0.311 ± 0.05 a.u.). We note that the values of KG are obtained by a sensitive extrapolation of the QMC results for systems with a finite number of electrons ($N=8$ and 12) to an infinite system. We do not exclude the possibility that their error bar is underestimated, or that there are other problems with their extrapolation procedure. Considering the consistency of our results, it is hard to believe that the band gaps will considerably increase when even higher-order contributions in W are included than the ones we have already taken into account. Moreover, in all cases we know of, RPA-GW band gaps starting from an LDA Green function are very close to the actual band gaps.

In summary, the main result of this paper is that, for the quasi-one-dimensional model semiconductor we studied, the band gap after systematic inclusion of all lowest-order corrections to the RPA polarizability and the GW self-energy is roughly the same as the RPA-GW band gap. For this it is

TABLE IV. Same as Table III, but for $A=0.25$.

	LDA	RPA-GW	Most complete
$k=0$	0.7882	0.7863 (-0.0289)	0.785 (-0.024)
$k=\pi/2a$	0.4023	0.4450 (-0.0325)	0.449 (-0.025)
$k=\pi/a$	0.0750	0.1836 (-0.0341)	0.193 (-0.035)

necessary to start from the LDA Green function. There are large cancellations between the lowest-order vertex and self-consistency corrections to P. To obtain a gap that is close to the RPA-GW band gap, however, it is also necessary to simultaneously include such corrections in M. Of course, we have only shown that this occurs when the *lowest-order* corrections in the screened interaction are included. Nevertheless, our expectation is that this principle is more general, although we do not yet have a clear understanding of it. In any case our results have shed an interesting light on the remarkable fact that non-self-consistent RPA-GW calculations in numerous materials have been so very successful. Presently, we are investigating whether the same trends occur in the real materials silicon and diamond.

ACKNOWLEDGMENTS

We thank Carl-Olof Almbladh and Ulf von Barth for useful discussions. This work has been supported in part by the European Community program Human Capital and Mobility through Contract No. CHRX-CT93-0337.

APPENDIX: EXPRESSIONS FOR VERTEX AND SELF-CONSISTENCY DIAGRAMS

In this appendix we give general expressions for the contributions to P and M depicted in Figs. 1 and 2, respectively. Using atomic units, the expression for the RPA polarizability, depicted by diagram RPA of Fig. 1, in energy-momentum space, is

$$P^{\mathrm{RPA}}_{K_1,K_2}(k,\epsilon)=2\sum_{Q_1,Q_2}\int_{1\mathrm{BZ}}\frac{dq_1}{2\pi}\int_{-\infty}^{\infty}\frac{d\epsilon_1}{2\pi i}G^0_{Q_1,Q_2}(q_1,\epsilon_1)G^0_{Q_2-K_2,Q_1-K_1}(q_1-k,\epsilon_1-\epsilon), \tag{A1}$$

where G^0 is a zeroth-order Green function. The factor of 2 comes from spin summation. K and Q denote reciprocal lattice vectors, the q_1 integral runs over the first Brillouin zone (1BZ), and the energy integrations are performed over the real energy axis. The expression for diagram V of Fig. 1, the lowest-order vertex correction to P, is

$$\begin{aligned}P^{V}_{K_1,K_2}(k,\epsilon)=-2\sum_{Q_{1\cdots 6}}\int_{1\mathrm{BZ}}\frac{dq_1}{2\pi}\frac{dq_2}{2\pi}\int_{-\infty}^{\infty}\frac{d\epsilon_1}{2\pi i}\frac{d\epsilon_2}{2\pi i}G^0_{Q_1,Q_2+Q_3}(q_1+q_2,\epsilon_1)G^0_{Q_3,Q_4}(q_2,\epsilon_1-\epsilon_2)G^0_{Q_4+K_2,Q_5}\\ \times(q_2+k,\epsilon_1-\epsilon-\epsilon_2)G^0_{Q_5+Q_6,Q_1+K_1}(q_1+q_2+k,\epsilon_1-\epsilon)W_{Q_2,Q_6}(q_1,\epsilon_2),\end{aligned} \tag{A2}$$

where W is the screened interaction. The expression for diagram SC1 of Fig. 1 is

$$\begin{aligned}P^{\mathrm{SC1}}_{K_1,K_2}(k,\epsilon)=2\sum_{Q_{1\cdots 6}}\int_{1\mathrm{BZ}}\frac{dq_1}{2\pi}\frac{dq_2}{2\pi}\int_{-\infty}^{\infty}\frac{d\epsilon_1}{2\pi i}\frac{d\epsilon_2}{2\pi i}G^0_{Q_1,Q_2}(q_1,\epsilon_1)G^0_{Q_2-Q_3,Q_5-Q_4}(q_1-q_2,\epsilon_1-\epsilon_2)\\ \times G^0_{Q_5,Q_6}(q_1,\epsilon_1)G^0_{Q_6-K_2,Q_1-K_1}(q_1-k,\epsilon_1-\epsilon)W_{Q_3,Q_4}(q_2,\epsilon_2).\end{aligned} \tag{A3}$$

For diagram SC2 of Fig. 1 we get the same expression as Eq. (7). Diagram SC3 of Fig. 1 represents

$$\begin{aligned}P^{\mathrm{SC2}}_{K_1,K_2}(k,\epsilon)=-2\sum_{Q_{1\cdots 6}}\int_{1\mathrm{BZ}}\frac{dq_1}{2\pi}\int_{-\infty}^{\infty}\frac{d\epsilon_1}{2\pi i}G^0_{Q_1,Q_2}(q_1,\epsilon_1)G^0_{Q_2-Q_3,Q_5-Q_4}(q_1,\epsilon_1)G^0_{Q_5,Q_6}(q_1,\epsilon_1)\\ \times G^0_{Q_6-K_2,Q_1-K_1}(q_1-k,\epsilon_1-\epsilon)V^{\mathrm{XC}}_{Q_3-Q_4}.\end{aligned} \tag{A4}$$

For diagram SC4 of Fig. 1 we get the same expression as Eq. (A4).

The GW self-energy is given by

$$M^{GW}_{K_1,K_2}(k,\epsilon)=-\sum_{Q_1,Q_2}\int_{1\mathrm{BZ}}\frac{dq_1}{2\pi}\int_{-\infty}^{\infty}\frac{d\epsilon_1}{2\pi i}G_{Q_1,Q_2}(q_1,\epsilon-\epsilon_1)W_{Q_1-K_1,Q_2-K_2}(k-q_1,\epsilon_1). \tag{A5}$$

The expression for diagram V of Fig. 2, the lowest-order vertex correction to the self-energy, is

$$\begin{aligned}M^{V}_{K_1,K_2}(k,\epsilon)=\sum_{Q_{1\cdots 6}}\int_{1\mathrm{BZ}}\frac{dq_1}{2\pi}\frac{dq_2}{2\pi}\int_{-\infty}^{\infty}\frac{d\epsilon_1}{2\pi i}\frac{d\epsilon_2}{2\pi i}G_{Q_3-Q_5,Q_4-Q_6}(q_1+q_2-k,\epsilon_1+\epsilon_2-\epsilon)\\ \times G_{Q_4,K_2-Q_2}(q_1,\epsilon_1)G_{K_1-Q_1,Q_3}(q_2,\epsilon_2)W_{Q_5,Q_2}(k-q_1,\epsilon_1-\epsilon)W_{Q_1,Q_6}(k-q_2,\epsilon_2-\epsilon).\end{aligned} \tag{A6}$$

The expression for diagram SC1 of Fig. 2 is

$$\begin{aligned}M^{\mathrm{SC1}}_{K_1,K_2}(k,\epsilon)=\sum_{Q_{1\cdots 6}}\int_{1\mathrm{BZ}}\frac{dq_1}{2\pi}\frac{dq_2}{2\pi}\int_{-\infty}^{\infty}\frac{d\epsilon_1}{2\pi i}\frac{d\epsilon_2}{2\pi i}G_{Q_1,Q_2}(q_1,\epsilon_1)G_{Q_3,Q_4}(q_2,\epsilon_2)G_{Q_5,Q_6}(q_1,\epsilon_1)\\ \times W_{Q_2-Q_3,Q_5-Q_4}(q_1-q_2,\epsilon_1-\epsilon_2)W_{K_2-Q_1,K_1-Q_6}(k-q_1,\epsilon-\epsilon_1).\end{aligned} \tag{A7}$$

The expression for diagram SC2 of Fig. 2 is

$$M^{\mathrm{SC2}}_{K_1,K_2}(k,\epsilon)=\sum_{Q_{1\cdots6}}\int_{1\mathrm{BZ}}\frac{dq_1}{2\pi}\int_{-\infty}^{\infty}\frac{d\epsilon_1}{2\pi i}G_{Q_4,K_1+Q_2}(q_1,\epsilon_1)G_{K_2+Q_1,Q_3}(q_1,\epsilon_1)V^{\mathrm{XC}}_{Q_3-Q_4}W_{-Q_1,-Q_2}(k-q_1,\epsilon-\epsilon_1). \quad \text{(A8)}$$

The expression for diagram SC3 of Fig. 2 is

$$M^{\mathrm{SC3}}_{K_1,K_2}=-2\sum_{Q_{1\cdots6}}\int_{1\mathrm{BZ}}\frac{dq_1}{2\pi}\frac{dq_2}{2\pi}\int_{-\infty}^{\infty}\frac{d\epsilon_1}{2\pi i}\frac{d\epsilon_2}{2\pi i}G_{Q_2,Q_3}(q_1,\epsilon_1)G_{Q_4,Q_5}(q_2,\epsilon_2)$$
$$\times G_{Q_6,Q_1+Q_2}(q_1,\epsilon_1)v_{Q_1,K_1-K_2}(0)W_{Q_3-Q_4,Q_6-Q_5}(q_1-q_2,\epsilon_1-\epsilon_2). \quad \text{(A9)}$$

Finally, the expression for diagram SC4 of Fig. 2 is

$$M^{\mathrm{SC4}}_{K_1,K_2}=-2\sum_{Q_{1\cdots4}}\int_{1\mathrm{BZ}}\frac{dq_1}{2\pi}\int_{-\infty}^{\infty}\frac{d\epsilon_1}{2\pi i}v_{Q_1,K_1-K_2}(0)G_{Q_2,Q_3}(q_1,\epsilon_1)G_{Q_4,Q_1+Q_2}(q_1,\epsilon_1)V^{\mathrm{XC}}_{Q_3-Q_4}. \quad \text{(A10)}$$

In the Q_1 summations in Eqs. (A9) and (A10) the case $Q_1=K_1-K_2$ should be excluded. As usual, the corresponding infinite contributions cancel against the infinite contributions from the interaction of the electrons with the positive background.

[1] H.J. de Groot, P.A. Bobbert, and W. van Haeringen, Phys. Rev. B **52**, 11 000 (1995).
[2] W. Knorr and R.W. Godby, Phys. Rev. Lett. **68**, 639 (1992).
[3] W. Knorr and R.W. Godby, Phys. Rev. B **50**, 1779 (1994).
[4] L. Hedin, Phys. Rev. **139**, A796 (1965).
[5] W. Kohn, Phys. Rev. **110**, 857 (1958).
[6] D.F. DuBois, Ann. Phys. (N.Y.) **7**, 174 (1959).
[7] D.F. DuBois, Ann. Phys. **8**, 24 (1959).
[8] D.J.W. Geldart and R. Taylor, Can. J. Phys. **48**, 155 (1970).
[9] D.J.W. Geldart and R. Taylor, Can. J. Phys. **48**, 167 (1970).
[10] P. Minnhagen, J. Phys. C **7**, 3013 (1974).
[11] G.D. Mahan and B.E. Sernelius, Phys. Rev. Lett. **62**, 2718 (1989).
[12] S. Hong and G.D. Mahan, Phys. Rev. B **50**, 8182 (1994).
[13] G. Mahan, Comments Condens. Mater. Phys. **16**, 333 (1994).
[14] E. Engel and S.H. Vosko, Phys. Rev. B **42**, 4940 (1990).
[15] R. Daling and W. van Haeringen, Phys. Rev. B **40**, 11 659 (1989).
[16] P.A. Bobbert and W. van Haeringen, Phys. Rev. B **49**, 10 326 (1994).
[17] C. Verdozzi, R.W. Godby, and S. Holloway, Phys. Rev. Lett. **74**, 2327 (1995).
[18] G.E. Engel, B. Farid, C.M.N. Nex, and N.H. March, Phys. Rev. B **44**, 13 356 (1991).